FIG. 4. Means of cell densities in the spiral ligament and types I–V ▶
fibrocyte areas following local saline or 3-NP application in the
apical, upper basal, and basal turns of cochleae. In the total area of
the spiral ligament, significant and dose-dependent decreases of cell
densities are found in the apical, upper basal, and basal portions of
cochleae (A). In the type I fibrocyte area, no significant decrease is
observed (B). Significant and dose-dependent loss of fibrocytes were
found in types II (C), III (D), IV (E), and V (F) areas. Asterisks indicate
significant differences to the control group at $p<0.05$ (ANOVA with
the Scheffe's test). Bars represent standard errors.

both Cx26 and Na,K-ATPase α (Spicer and Schulte
1991; Schulte and Steel 1994; Xia et al. 1999).

Degeneration of the stria vascularis

Light microscopic examination of the HE-stained
samples revealed no significant degeneration of the
SV following saline, 1, or 3 mM 3-NP application
(Fig. 5A–C). Immunostaining for Na,K-ATPase α also
demonstrated no alteration in its expression in the SV
among specimens treated with saline, 1, or 3 mM 3-NP
(Fig. 5I–K). In addition, the expression of Cx26 in the
basal cell area of the SV in these specimens remained
similar to controls (Fig. 5E–G). The findings indicat-
ing no significant damage in the SV following 1 or
3 mM 3-NP application were supported by a quanti-
tative assessment of the SV ratio showing no signifi-
cant differences in each portion of cochleae between
these experimental groups (Fig. 6). The cochleae
injected with 5 or 10 mM 3-NP often exhibited the
atrophy of the SV (Fig. 5D). In the apical and mid-
basal turns of the cochleae, a quantitative assessment
of the SV ratio demonstrated no significant decrease
among the experimental groups, while in the basal
portion of the cochleae, significant decreases of the
SV area were identified in both 5 and 10 mM 3-NP-
treated cochleae (Fig. 6). Although the expression of
Na,K-ATPase α and Cx26 was still observed in the SV
following 5 or 10 mM 3-NP application, their expres-
sion patterns were altered (Fig. 5H, L) in comparison
with those in controls.

Degeneration of the organ of Corti

Immunohistochemistry for myosin VIIa and staining
with phalloidin in whole mounts of the organ of Corti
demonstrated no significant loss of IHCs in cochleae

◀ FIG. 3. Low magnification images of mid-modiolar sections of
controls, 1, 3, 5, and 10 mM 3-NP treated cochleae. Hematoxylin
and eosin staining (A, C, E, G, I) and immunostaining for Na,K-
ATPase α (B, D, F, H, J) show the loss of fibrocytes in the inferior
portion of cochleae with the loss of immunoreactivity for Na,K-
ATPase α (arrows). The loss of immunoreactivity for Na,K-ATPase α in
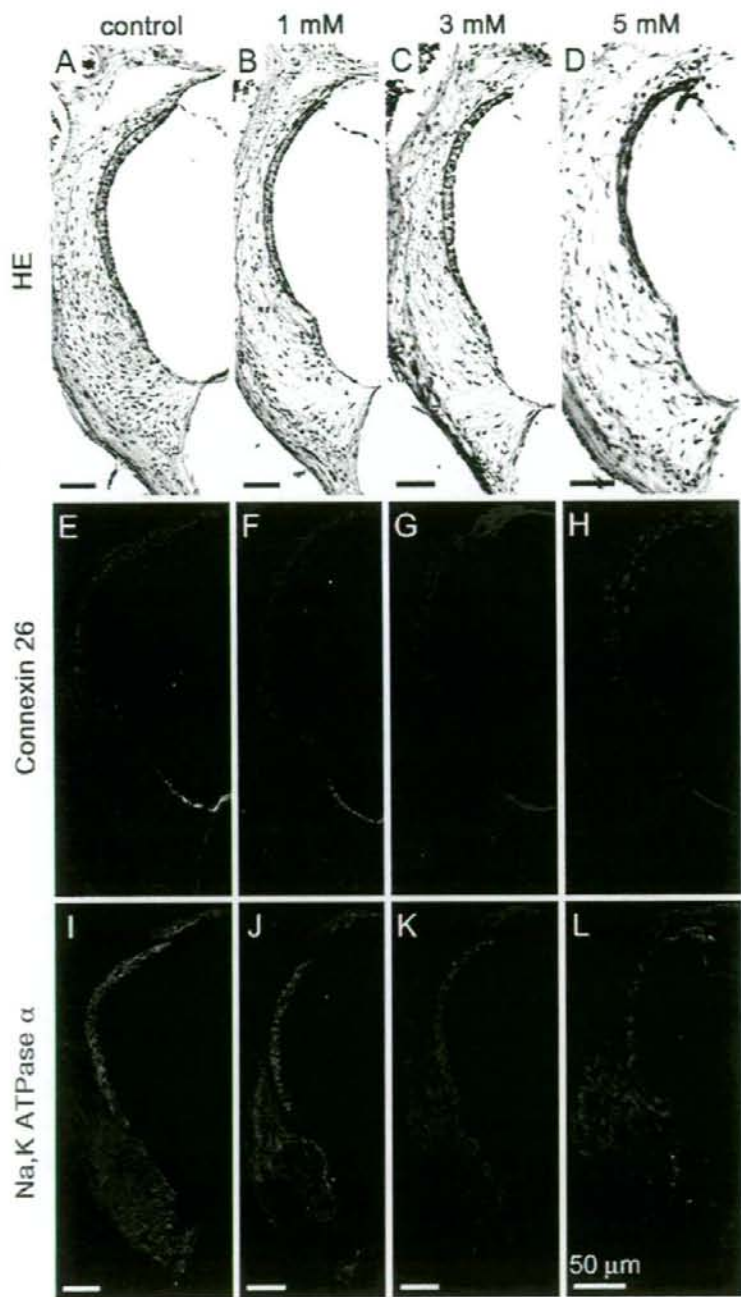spiral ganglions in the apical and upper basal portions of cochleae
(asterisks).
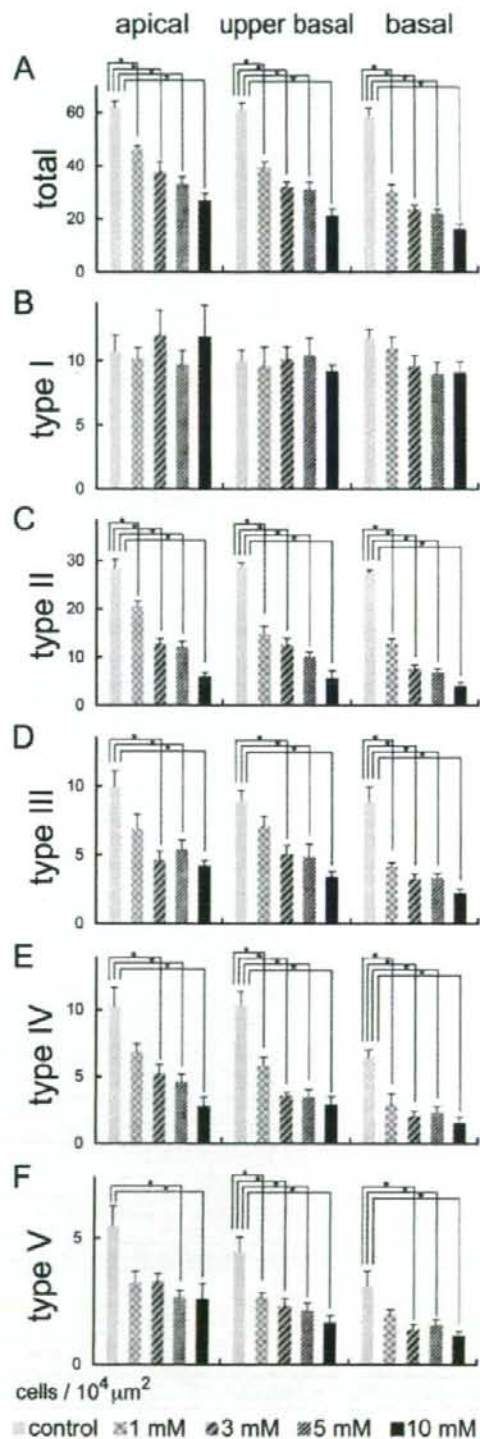
FIG. 5. Expressions of connexin 26 and Na,K-ATPase α in the cochlear lateral wall following local saline or 3-NP application. HE staining sections next to immunostaining sections (**A–D**) demonstrate dose-dependent decreases of fibrocytes notably in the inferior portion of the spiral ligament, and the atrophy of the stria vascularis in the specimen damaged by 5 mM 3-NP (**D**). Specimens damaged by 1 (**F, J**), 3 (**G, K**) or 5 mM 3-NP (**H, L**) exhibit a decline in expressions of connexin 26 and Na,K-ATPase α in the inferior portion of the spiral ligament. Both expressions in the stria vascularis are disarranged in the specimen damaged by 5 mM 3-NP (**H, L**).
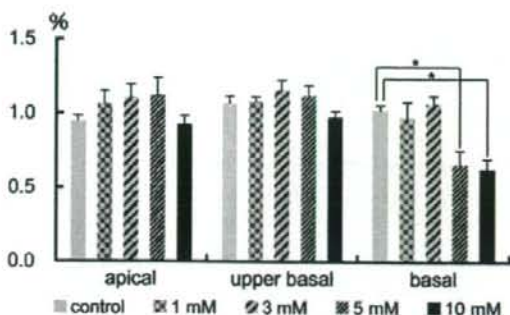
FIG. 6. Means of the SV ratios following local saline or 3-NP application in the apical, upper basal, and basal turns of cochleae. Significant decreases in the SV ratio are found in the basal turn of cochleae injected with 5 and 10 mM 3-NP ($^*p<0.05$, ANOVA with the Scheffe's test).

injected with 1, 3, or 5 mM 3-NP (Fig. 7A–D). The cochleae injected with 10 mM 3-NP exhibited severe loss of IHCs in each portion of cochleae (Fig. 7D). The cochleae injected with 5 or 10 mM of 3-NP exhibited severe degeneration of OHCs in each turn of cochleae (Fig. 7E). In cochlear specimens damaged by 3 mM 3-NP, a significant loss of OHCs was observed

in the basal portion of cochleae (Fig. 7C, E), while in the apical portion, OHCs were well maintained (Fig. 7E). Local application of 1 mM 3-NP induced no significant loss of OHCs (Fig. 7B, E).

Degeneration of the spiral ganglion

The cochleae injected with 1 mM 3-NP exhibited no degeneration of SGNs in any of the turns of the cochlea (Fig. 8A, B, G). In the animals injected with 3 mM 3-NP, degeneration of the SGN was not observed in the basal portion of the cochleae (Fig. 8D), while in the upper basal and apical portions, severe degeneration of the SGN was found (Fig. 8C, G). The cochleae damaged by 5 mM of 3-NP exhibited severe degeneration in the apical and upper basal portions (Fig. 8E, G), while SGNs in the basal portion of cochleae were preserved (Fig. 8F). After application of 10 mM of 3-NP, severe degeneration of the SGN was observed in all the turns of the cochleae (Fig. 8G). In contrast to patterns of degeneration in the SL, the SV, and the organ of Corti, there was a trend of increasing severity of SGN degeneration from the base to the apex in the cochleae.
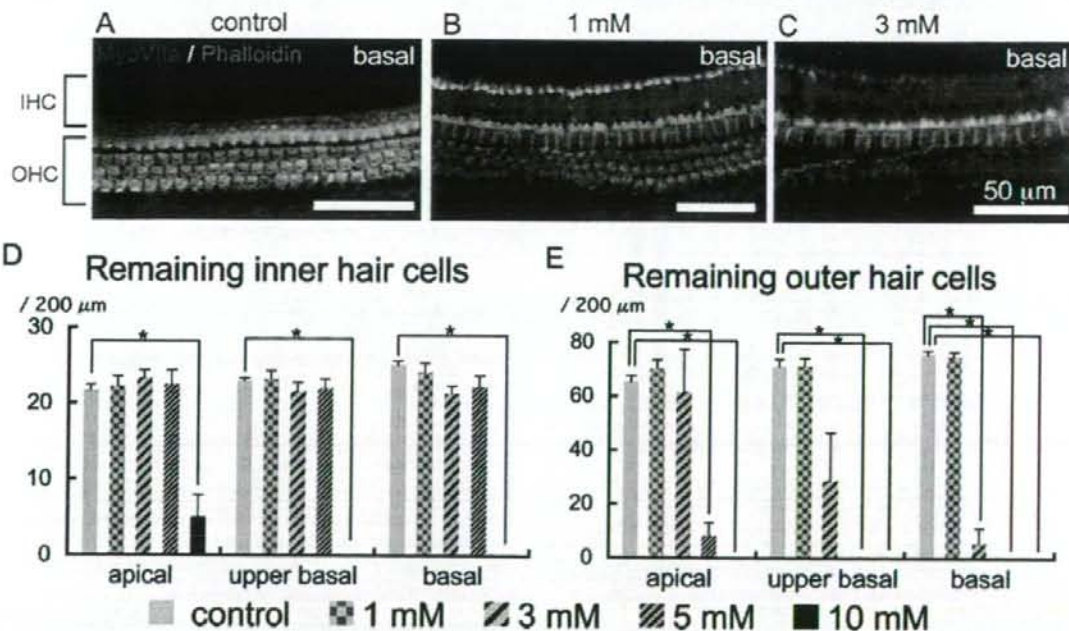

FIG. 7. Degeneration of the organ of Corti following local saline or 3-NP application. The control specimen treated with saline (A) shows a single row of inner hair cells (IHC) and three rows of outer hair cells (OHC) in the basal turn of the cochlea. In the basal turn of the cochlea injected with 1 mM 3-NP (B), IHC and OHC are well preserved, while severe OHC loss is found in the basal turn of the cochlea injected with 3 mM 3-NP (C). Means of remaining IHC are shown in (D), and those of remaining OHC are in E. Asterisks indicate significant differences to the control group at $p<0.05$ (ANOVA with the Scheffe's test). Bars in D, E represent standard errors.
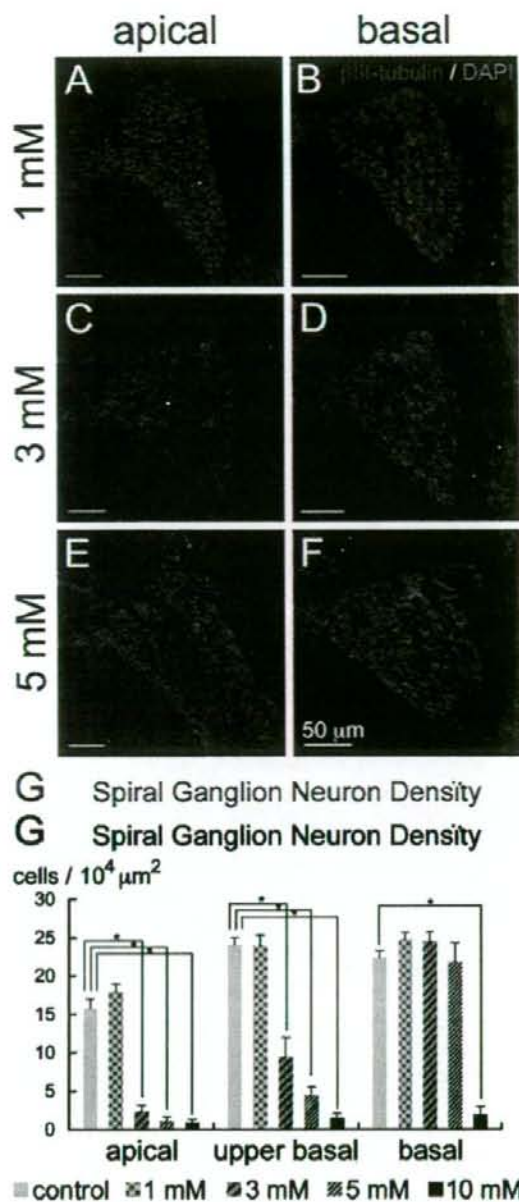
apical   basal

FIG. 8. Degeneration of the spiral ganglion neurons following local saline or 3-NP application. Immunostaining for βIII-tubulin (*red*) and nuclear staining with DAPI (*blue*) demonstrates no degeneration of spiral ganglion neurons in the apical (A) or basal (B) turn in the cochlea injected with 1 3-NP. In the cochlea injected with 3 (**C, D**) and 5 mM 3-NP (**E, F**), severe degeneration of spiral ganglion neurons is observed in the apical turn, while spiral ganglion neurons in the basal turn are preserved. Means of the densities of spiral ganglion neurons are shown in **G**. *Asterisks* indicate significant differences to the control group at $p < 0.05$ (ANOVA with the Scheffe's test). *Bars* in G represent standard errors.

DISCUSSION

The present study demonstrated that there was a dose-dependent degeneration of the mouse cochlea after a local application of 3-NP, which is an inhibitor of succinate dehydrogenase and causes ATP depletion. Local application of 5 or 10 mM 3-NP resulted in extensive and severe degeneration of the cochleae that led to severe functional loss. This indicated that the animals injected with 5 or 10 mM 3-NP were not suitable for experiments designed to develop an injury model to assess therapeutic interventions for the treatment of SL degeneration. In the animals injected with 1 mM 3-NP, there were significant ABR threshold shifts along with significant reductions of the EP. Histologically, selective degeneration of the SL was found with this dose, which is preferable for an animal model intended to investigate regeneration of the SL fibrocytes. However, a significant elevation of ABR thresholds was found only at 40 kHz, and the loss of the EP was less than 20 mV, which would make it difficult to show significant functional improvements by new therapeutic interventions using this dose. The application of 3 mM 3-NP induced moderate ABR threshold shifts with an approximate 50% reduction of the EP, making this model more suitable for investigations designed to assess SL regeneration and monitor functional recovery. However, the animals injected with 3 mM 3-NP exhibited not only SL degeneration but also degeneration of the SGN and the organ of Corti in particular regions of the cochlea. Therefore, if complete regeneration of SL fibrocytes is achieved by new therapeutic manipulations, ABR thresholds may not recover completely. However, recovery of the EP may be a useful measure of functional recovery promoted by SL regeneration, and partial recovery of ABR thresholds can be expected.

In the present study, a significant loss of SL fibrocytes was found following local 3-NP application in a dose-dependent manner. The severity of SL degeneration increased as a gradient from the apex to the base of the cochlea. Significant decreases of type II–V fibrocytes were observed in a dose-dependent manner, while no significant loss of type I fibrocytes was found. Among type II–V fibrocytes, type II fibrocytes are most vulnerable to 3-NP because 1 mM 3-NP application caused a significant loss of fibrocytes in the apical portion only in the type II fibrocytes area (Fig. 4). It is well known that C56BL/6 mice have an age-related hearing loss beginning at a very early age (Mikaelian et al. 1974). In parallel to progress in hearing loss, a loss of SL fibrocytes occurring in the type I, II, and IV areas can be observed as early as 12 weeks of age in this strain (Hequembourg and Liberman 2001). However, since we used age-matched, sham-operated cochleae as the

controls in the present study, age-related alterations in cell densities of SL fibrocytes have been accounted for and the remaining losses are attributed to toxicity. In gerbils, age-related degeneration of the type II fibrocytes, which express Na,K-ATPase, is closely associated with the reduction of the EP (Schulte and Schmiedt 1992; Spicer and Schulte 2002). Therefore, a significant loss of type II fibrocytes observed in the present study may play a critical role in significant reduction of the EP.

Aging and noise are included in common causes for SNHL, and both can induce SL degeneration. In aged C57/BL6 mice, severe loss of SL fibrocytes was found in the type I and IV areas rather than the type II area (Hequembourg and Liberman 2001). A loss of type II fibrocytes due to aging is predominant in the basal portion of the cochlea, which is similar to the present findings. Acoustic overstimulation induces the loss of SL fibrocytes in the type II and IV areas of cochlear regions corresponding to frequencies that show significant ABR threshold shifts in C57/BL6 mice (Hirose and Liberman 2003). The present results also demonstrated severe degeneration of type II and IV fibrocytes following local 3-NP application. These findings indicate the vulnerability of type II and IV fibrocytes of C57/BL6 mice.

A 3-NP solution injected from the PSCC should first reach the basal portion of the cochlea and then spread to the apex. Hence, the concentration of 3-NP in different regions of the cochlea should differ. The concentration of 3-NP in the basal portion of cochleae is expected to be higher than the apical portion. Type II fibrocytes have abundant mitochondria (Henson and Henson 1988; Hirose and Liberman 2003), indicating high energy demands of this cell type. Therefore, more severe degeneration of type II fibrocytes in the basal than apical portion of cochleae observed at lower doses in the present study may reflect a higher concentration. OHCs, on the other hand, have a relatively low volume density of mitochondria and lack appreciable Na,K-ATPase, suggesting that OHCs may be resistant to 3-NP toxicity. However, in this study, severe degeneration of OHCs was found in the basal portion of the cochleae. One possible explanation for OHC degeneration is secondary degeneration of OHCs due to disruption of the gap junction networks in the cochlea. Degeneration of SL fibrocytes by 3-NP results in the destruction of connective tissue gap junction networks of the fibrocytes in the lateral wall. Gap junctions are responsible not only for anionic molecule permeability but also for metabolic communications (Zhang et al. 2005; Zhao 2005). Therefore, destruction of gap junctions may cause metabolic disorders in OHCs leading to OHC death. Actually, the disruption of the epithelial gap junction network between supporting cells in the organ of Corti due to genetic disorders results in secondary degeneration of OHCs (Cohen-Salmon et al. 2002). In addition, even if the epithelial gap junction network remains intact, OHCs could suffer from acute potassium ion intoxication owing to the loss of type II fibrocytes.

In contrast to SL fibrocytes and OHCs, the severity of SGN degeneration that was observed following the 3-NP application increased in a gradient from the basal to the apical portion of the cochleae, although the concentration of 3-NP in the apical portion of the cochleae may be lower than that in the basal portion. In the current study, HCs in the apical portion of the cochleae were well preserved, indicating that the SGN degeneration in the apical portion was not caused by depletion of the trophic supports from HCs. On the other hand, several studies using the endolymphatic hydrops model (Nadol et al. 1995; Bixenstine et al. 2008), which is a model for Ménière's disease, and of age-related pathological changes in the cochlea (Schulte and Schmiedt 1992; Suryadevara et al. 2001) have demonstrated predominant losses of the SGN in the apical portion of the cochleae, suggesting the vulnerability of SGNs in this region. In gerbils, loss of SGN due to aging is observed parallel to the decrease of the EP (Suryadevara et al. 2001). Therefore, reduction of the EP due to SL degeneration might contribute to SGN degeneration demonstrated in the present study.

In conclusion, the present findings demonstrate that local 3-NP application causes functional and histological degeneration of the mouse cochleae in a dose-dependent manner. An injection of 1 mM 3-NP into the PSCC induces selective degeneration of the SL fibrocytes along with a significant reduction of the EP; however, the loss of the EP was limited to 20 mV. The animals injected with 3 mM 3-NP demonstrated significant ABR threshold shifts with an approximate 50% reduction of the EP, which is suitable for investigations designed to test the feasibility of therapeutic interventions for functional recovery of the SL. In the near future, we are planning on using these models to examine the efficacy of cell transplantation for histological and functional regeneration of the SL.

ACKNOWLEDGMENTS

the Ministry of Health, Labor and Welfare of Japan and by a grant from the Takeda Science Foundation.

REFERENCES

BIXENSTINE PJ, MANIGLIA MP, VASANJI A, ALAGRAMAM KN, MEGERIAN CA. Spiral ganglion degeneration patterns in endolymphatic hydrops. Laryngoscope. 118:1217–1223, 2008.

COHEN-SALMON M, OTT T, MICHEL V, HARDELIN JP, PERFETTINI I, EYBALIN M, WU T, MARCUS DC, WANGEMANN P, WILLECKE K, PETIT C. Targeted ablation of connexin26 in the inner ear epithelial gap junction network causes hearing impairment and cell death. Curr. Biol. 12:1106–1111, 2002.

HENSON MM, HENSON OW. Tension fibroblasts and the connective tissue matrix of the spiral ligament. Hear. Res. 35:237–258, 1988.

HEQUEMBOURG S, LIBERMAN MC. Spiral ligament pathology: a major aspect of age-related cochlear degeneration in C57BL/6 mice. J. Assoc. Res. Otolaryngol. 2:118–129, 2001.

HIROSE K, LIBERMAN MC. Lateral wall histopathology and endocochlear potential in the noise-damaged mouse cochlea. J. Assoc. Res. Otolaryngol. 4:339–352, 2003.

HOYA N, OKAMOTO Y, KAMIYA K, FUJII M, MATSUNAGA T. A novel animal model of acute cochlear mitochondrial dysfunction. Neuroreport. 15:1597–1600, 2004.

IGUCHI F, NAKAGAWA T, TATEYA I, ENDO T, KIM TS, DONG Y, KITA T, KOJIMA K, NAITO Y, OMORI K, ITO J. Surgical techniques for cell transplantation into the mouse cochlea. Acta Otolaryngol. 551:43–47, 2004.

IZUMIKAWA M, MINODA R, KAWAMOTO K, ABRASHKIN KA, SWIDERSKI DL, DOLAN DF, BROUGH DE, RAPHAEL Y. Auditory hair cell replacement and hearing improvement by Atoh1 gene therapy in deaf mammals. Nat. Med. 11:271–276, 2005.

KUSUNOKI T, CUREOGLU S, SCHACHERN PA, BABA K, KARIYA S, PAPARELLA MM. Age-related histopathologic changes in the human cochlea: a temporal bone study. Otolaryngol. Head Neck Surg. 131:897–903, 2004.

LEE JE, NAKAGAWA T, KIM TS, IGUCHI F, ENDO T, DONG Y, YUKI K, NAITO Y, LEE SH, ITO J. A novel model for rapid induction of apoptosis in spiral ganglions of mice. Laryngoscope. 113:994–999, 2003.

MAHMUD MR, KHAN AM, NADOL JB. Histopathology of the inner ear in unoperated acoustic neuroma. Ann. Otol. Rhinol. Laryngol. 112:979–986, 2003.

MIKAELIAN DO, WARFIELD D, NORRIS O. Genetic progressive hearing loss in the C57-bl16 mouse. Relation of behavioral responses to cochlear anatomy. Acta Otolaryngol. 77:327–334, 1974.

MINOWA O, IKEDA K, SUGITANI Y, OSHIMA T, NAKAI S, KATORI Y, SUZUKI M, FURUKAWA M, KAWASE T, ZHENG Y, OGURA M, ASADA Y, WATANABE K, YAMANAKA H, GOTOH S, NISHI-TAKESHIMA M, SUGIMOTO T, KIKUCHI T, TAKASAKA T, NODA T. Altered cochlear fibrocytes in a mouse model of DFN3 nonsyndromic deafness. Science. 285:1408–1411, 1999.

NADOL JB, JR, ADAMS JC, KIM JR. Degenerative changes in the organ of Corti and lateral cochlear wall in experimental endolymphatic hydrops and human Ménière's disease. Acta Otolaryngol. 519:47–59, 1995.

NAKAGAWA T, KIM TS, MURAI N, ENDO T, IGUCHI F, TATEYA I, YAMAMOTO N, NAITO Y, ITO J. A novel technique for inducing local inner ear damage. Hear. Res. 176:122–127, 2003.

OHLEMILLER KK. Age-related hearing loss: the status of Schuknecht's typology. Curr. Opin. Otolaryngol. Head Neck Surg. 12:439–443, 2004.

OKAMOTO Y, HOYA N, KAMIYA K, FUJII M, OGAWA K, MATSUNAGA T. Permanent threshold shift caused by acute cochlear mitochondrial dysfunction is primarily mediated by degeneration of the lateral wall of the cochlea. Audiol. Neurootol. 10:220–233, 2005.

OKANO T, NAKAGAWA T, ENDO T, KIM TS, KITA T, TAMURA T, MATSUMOTO M, OHNO T, SAKAMOTO T, IGUCHI F, ITO J. Engraftment of embryonic stem cell-derived neurons into the cochlear modiolus. Neuroreport. 16:1919–1922, 2005.

OKANO T, NAKAGAWA T, KITA T, ENDO T, ITO J. Cell-gene delivery of brain-derived neurotrophic factor to the mouse inner ear. Mol. Ther. 14:866–871, 2006.

SCHULTE BA, SCHMIEDT RA. Lateral wall Na,K-ATPase and endocochlear potentials decline with age in quiet-reared gerbils. Hear. Res. 61:35–46, 1992.

SCHULTE BA, STEEL KP. Expression of alpha and beta subunit isoforms of Na,K-ATPase in the mouse inner ear and changes with mutations at the Wv or Sld loci. Hear Res. 78:65–76, 1994.

SHIGA A, NAKAGAWA T, NAKAYAMA M, ENDO T, IGUCHI F, KIM TS, NAITO Y, ITO J. Aging effects on vestibulo-ocular responses in C57BL/6 mice: comparison with alteration in auditory function. Audiol. Neurootol. 10:97–104, 2005.

SPICER SS, SCHULTE BA. Differentiation of inner ear fibrocytes according to their ion transport related activity. Hear. Res. 56:53–64, 1991.

SPICER SS, SCHULTE BA. Spiral ligament pathology in quiet-aged gerbils. Hear. Res. 172:172–185, 2002.

SURYADEVARA AC, SCHULTE BA, SCHMIEDT RA, SLEPECKY NB. Auditory nerve fibers in young and quiet-aged gerbils: morphometric correlations with endocochlear potential. Hear. Res. 161:45–53, 2001.

SUZUKI T, NOMOTO Y, NAKAGAWA T, KUWAHATA N, OGAWA H, SUZUKI Y, ITO J, OMORI K. Age-dependent degeneration of the stria vascularis in human cochleae. Laryngoscope. 116:1846–1850, 2006.

VASAMA JP, LINTHICUM FH. Meniere's disease and endolymphatic hydrops without Meniere's symptoms: temporal bone histopathology. Acta Otolaryngol. 119:297–301, 1999.

XIA AP, KIKUCHI T, HOZAWA K, KATORI Y, TAKASAKA T. Expression of connexin 26 and Na,K-ATPase in the developing mouse cochlear lateral wall: functional implications. Brain Res. 846:106–111, 1999.

XIA AP, KIKUCHI T, MINOWA O, KATORI Y, OSHIMA T, NODA T, IKEDA K. Late-onset hearing loss in a mouse model of DFN3 nonsyndromic deafness: morphologic and immunohistochemical analyses. Hear. Res. 166:150–158, 2002.

ZHANG Y, TANG W, AHMAD S, SIPP JA, CHEN P, LIN X. Gap junction-mediated intercellular biochemical coupling in cochlear supporting cells is required for normal cochlear functions. Proc. Natl. Acad. Sci. U.S.A. 102:15201–15206, 2005.

ZHAO HB. Connexin26 is responsible for anionic molecule permeability in the cochlea for intercellular signalling and metabolic communications. Eur. J. Neurosci. 21:1859–1868, 2005.

Hydrogen protects auditory hair cells from free radicals

Yayoi S. Kikkawa, Takayuki Nakagawa, Rie T. Horie and Juichi Ito

Reactive oxygen species (ROS) play a role in the degeneration of auditory hair cells because of aging, noise trauma, or ototoxic drugs. Hydrogenation is a fundamental reduction/deoxidation reaction in living organisms. This study thus examined the potential of hydrogen to protect auditory hair cells from ROS-induced damage. To generate ROS, we applied antimycin A to explant cultures of auditory epithelia, and examined the effect of hydrogen on the protection of hair cells against ROS. Incubation with a hydrogen-saturated medium significantly reduced ROS generation and subsequent lipid peroxidation in the auditory epithelia, leading to increased survival of the hair cells. These findings show the potential of hydrogen to protect auditory hair cells from ROS-induced

damage. *NeuroReport* 00:000–000 © 2009 Wolters Kluwer Health | Lippincott Williams & Wilkins.

Department of Otolaryngology–Head and Neck Surgery, Graduate School of Medicine, Kyoto University, Kyoto, Japan

Correspondence to Dr Takayuki Nakagawa, MD, PhD, Department of Otolaryngology–Head and Neck Surgery, Graduate School of Medicine, Kyoto University, Kawahara-cho 54, Shogoin, Sakyo-ku, Kyoto 606-8507, Japan
Tel: +81 75 751 3346; fax: +81 75 751 7225;
e-mail: tnakagawa@ent.kuhp.kyoto-u.ac.jp

Introduction

Hearing disorders affect nearly 10% of the world population. The common causes of sensorineural hearing loss because of cochlear injury are aging, hereditary disorders, noise trauma, and ototoxic drugs. The mechanisms underlying cochlear injury are still not completely known. However, numerous studies have suggested that they involve the production of reactive oxygen species (ROS), which cause cellular injury in the cochlea resulting in sensorineural hearing loss [1–4]. Although they are probably intended to fight against invasive pathogens, ROS seem to produce substantial collateral damage through DNA strand breaks, lipid and protein oxidation [5–7].

Hydrogenation is a fundamental reduction/deoxidation reaction in living organisms. Many reduction processes in the body involve electron transfer from molecular hydrogen. This molecule was recently established as an antioxidant that selectively reduces the hydroxyl radical, and was shown to decrease the cerebral infarction volume after ischemia in rats [8]. Subsequently, protective effects of hydrogen gas have been demonstrated in a mouse model for hepatic injury [9] and in a rat model for myocardial infarction [10]. In the nervous system, hydrogen-rich water was shown to prevent superoxide formation in mouse brain slices [11], and to prevent stress-induced impairments in learning tasks during chronic physical restraint in mice [12]. Moreover, a clinical study showed that consuming hydrogen-rich pure water improves lipid and glucose metabolism in type 2 diabetes patients [13].

The ex-vivo study reported here tested the hypothesis that molecular hydrogen, hydrogen gas, protects against cochlear impairment by scavenging free radicals. We

initially generated in situ ROS in the cochlea using an inhibitor of mitochondrial respiratory chain complex III, antimycin A, and showed that they caused direct damage to the hair cells. Then, using a hydrogen (hydrogen gas)-saturated culture media, we demonstrated that hydrogen gas alleviated ROS-induced ototoxicity, suggesting that hydrogen gas has the potential to act as an antioxidant for the treatment of cochlear damage. We also evaluated the generated hydroxyl radicals by fluorescence emission of 2-[6-(4′-hydroxy)phenoxy-3H-xanthen-3-on-9-yl] benzoate (HPF) and lipid peroxidation by immunohistochemistry for 4-hydroxynonenal (HNE).

Materials and methods

Animals

The ICR mice (Japan SLC, Hamamatsu, Japan) used in this study were cared for in the Institute of Laboratory Animals of the Kyoto University Graduate School of Medicine. The Animal Research Committee of the Kyoto University Graduate School of Medicine approved all experimental protocols, which were performed in accordance with the National Institutes of Health Guidelines for the Care and Use of Laboratory Animals.

Cochlear explant culture

Postnatal day 2 (P2) ICR mice were deeply anesthetized with diethyl ether and decapitated. The temporal bones were dissected, and the cochleae were freed from the surrounding tissue and placed in 0.01 M phosphate-buffered saline (PBS; pH 7.4). After removing the cochlear lateral wall, the auditory epithelia were dissected from the cochlear modiolus. The tissue samples were then placed on glass-mesh inserts (Falcon, Billerica, Massachusetts, USA) and cultured initially in serum-free

modified Eagle's medium (MEM; Invitrogen, Eugene, Oregon, USA), supplemented with 3 g/l glucose (Wako Pure Chemicals, Osaka, Japan) and 0.3 g/l penicillin G (Wako), for 24 h at 37°C in a humidified (95%) air: 5% atmospheric CO_2. In total, 20 cochlear explants were used in a single culture, and at least three independent cultures were performed for each condition. As the hair cells in the apex are resistant to free radicals [14], the basal turns of the cochlea were used in this study.

Antimycin A application
The explants were transferred to medium containing antimycin A (Sigma-Aldrich, St Louis, Missouri, USA) at concentrations of 0.1, 1, or 10 µg/ml, with six to nine cochleae incubated at each concentration. The cultures were maintained for 24 h. At the end of the culture period, the samples were fixed for 15 min in 4% paraformaldehyde in 0.1 M phosphate buffer (pH 7.4), and then provided for immunostaining for myosin VIIa to evaluate the number of surviving hair cells. The specimens were incubated with primary rabbit polyclonal antibodies against myosin VIIa (1 : 500; Proteus Bioscience Inc., Ramona, California, USA). Alexa-Fluor 568 goat anti-rabbit IgG (1 : 200; Invitrogen) was used as the secondary antibody. Specimens were then incubated in Alexa-Fluor 488-conjugated phalloidin (1 : 250; Invitrogen) to label F-actin. The specimens were examined with a Leica TCS-SP2 laser-scanning confocal microscope (Leica Microsystems Inc., Wetzlar, Germany). To quantify the hair-cell loss in the cochlea after the different treatments, inner hair cells (IHCs) and outer hair cells (OHCs) were counted over a 100-µm-long stretch of the auditory epithelia, in two separate regions of the basal turn in each culture (totaling 200 µm). For each treatment, six to nine cultures were evaluated.

Hydrogen treatment
To assess the efficacy of hydrogen gas for cochlear protection, explants were cultured initially in an airtight box (Chopla Industries, Inazawa, Japan) with reduced-CO_2-dependence media, MEM, and Leivovitz's L-15 media (Invitrogen) mixed in a 1 : 1 ratio [15], supplemented with 3 g/l glucose and 0.3 g/l penicillin G, at 37°C in a humidified (100%) atmospheric air. After 24 h, the medium was changed to one containing antimycin A at a concentration of 0.1, 1 or 10 µg/l, with or without hydrogen gas for another 24 h. Hydrogen gas was dissolved directly into the media, and a high content of dissolved hydrogen (1.3 ± 0.1 mg/l) was confirmed using a hydrogen electrode (Model M-10B2; Able Corporation, Tokyo, Japan). The pH of the culture media without hydrogen gas was 7.18 ± 0.02, and that of the culture media with hydrogen gas was 7.52 ± 0.02. The prepared media were used for culture within 30 min. At the end of the experiments, the explants were fixed and provided for histological analysis to evaluate hair-cell survival. Between six and 12 cochleae were used for each condition.

Detection of reactive oxygen species by fluorescent indicators
The cochlear explants were treated with 30 µM HPF (Daiichi Pure Chemicals Co., Tokyo, Japan) for 20 min to detect cellular hydroxyl radicals. Fluorescent images were captured with a Leica TCS-SP2 confocal microscope using excitation and emission filters of 488 and 510 nm, respectively. All images were taken with the same laser intensity, detector gain, and offset values. Fluorescent signals were quantified from two separate OHC regions of the basal turns, each of which was 1250 µm^2 (50 × 25 µm), using Image J software (http://rsb.info.nih.gov/ij/; NIH, Bethesda, MD). Intensity measurements were expressed relative to the levels in the control samples.

Lipid-peroxidation assay
Lipid peroxidation was assessed in cultures treated with antimycin A, in the presence or absence of hydrogen gas, by measuring the expression of HNE immunohistochemically. Explants were labeled with mouse anti-HNE monoclonal antibody (1 : 8; Oxis Research, Portland, Oregon, USA) and fluorescein horse anti-mouse immunoglobulin G (1 : 250; Vector Laboratories, Burlingame, California, USA) as the primary and secondary antibodies, respectively. Specimens were then counterstained with Alexa 568 phalloidin (1 : 250; Invitrogen). All images were taken with the same exposure and shutter speed. The green fluorescence intensity was measured in the same area using Image J software. Intensity measurements were expressed relative to the levels in the control samples.

Fig. 1
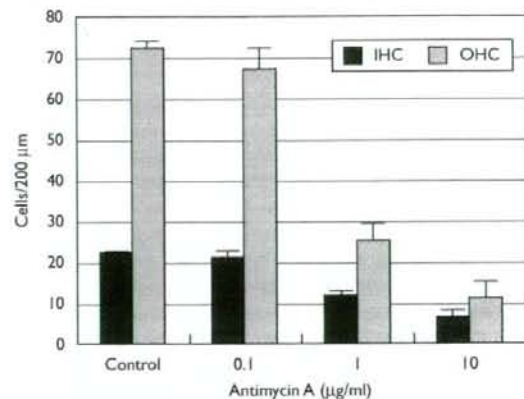
Antimycin A induced dose-dependent auditory hair-cell loss. The graph shows the relationship between the antimycin A concentration and the hair-cell count following 24-h culture. The inner hair cells (IHCs) and outer hair cells (OHCs) were counted in 200-µm-length regions from each cochlea. The hair-cell densities decreased systematically as the antimycin A concentration increased. Bars represent standard errors.

Statistical analysis

The overall effects on the hair-cell number, and the HPF and HNE staining intensities, were analyzed by two-way factorial analysis of variance (ANOVA) using the Statcel2 application (OMS Publishing, Saitama, Japan). *P* values less than 0.05 were considered to be statistically significant. For interactions that were found to be significant, multiple paired comparisons were analyzed using the Tukey–Kramer test.

Results

Antimycin A induced dose-dependent hair-cell loss

Initially, we established the dose–response relationship between the antimycin A concentration and its toxic effect on hair cells. The addition of 1 μg/ml antimycin A to cultures for 24 h significantly reduced the hair-cell numbers in both the IHC and OHC regions, with the effect being more severe in the latter (Fig. 1). The

addition of 1 μg/ml antimycin A destroyed 46.2 ± 4.6% of the IHCs and 65.6 ± 5.8% of the OHCs. The hair-cell density decreased depending on the concentrations of antimycin A and few could be detected in the auditory epithelia cultured in 10 μg/ml antimycin A (Fig. 2g).

Protective effect of hydrogen supplementation

Next, we assessed the potential of hydrogen to protect against antimycin-induced ototoxicity by administering 0, 0.1, 1, or 10 μg/ml antimycin to samples cultured in hydrogen-saturated media in an airtight environment. The addition of hydrogen markedly increased both IHC and OHC survival, with a substantial number of hair cells surviving even at the highest antimycin A dose (Figs 2 and 3). Two-way ANOVA showed that hydrogen gas had a significant effect on the numbers of surviving IHCs and OHCs ($P = 0.00305$ and $P = 0.00016$, respectively). Tukey–Kramer tests for multiple paired comparisons
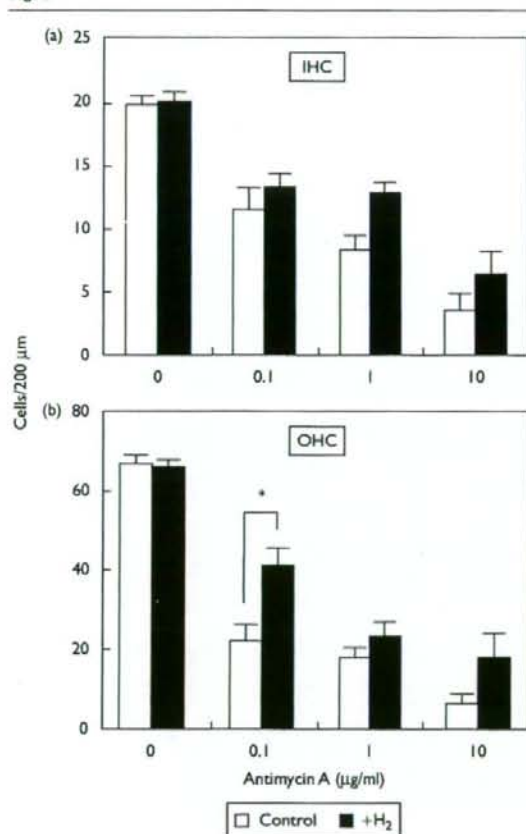
Fig. 2
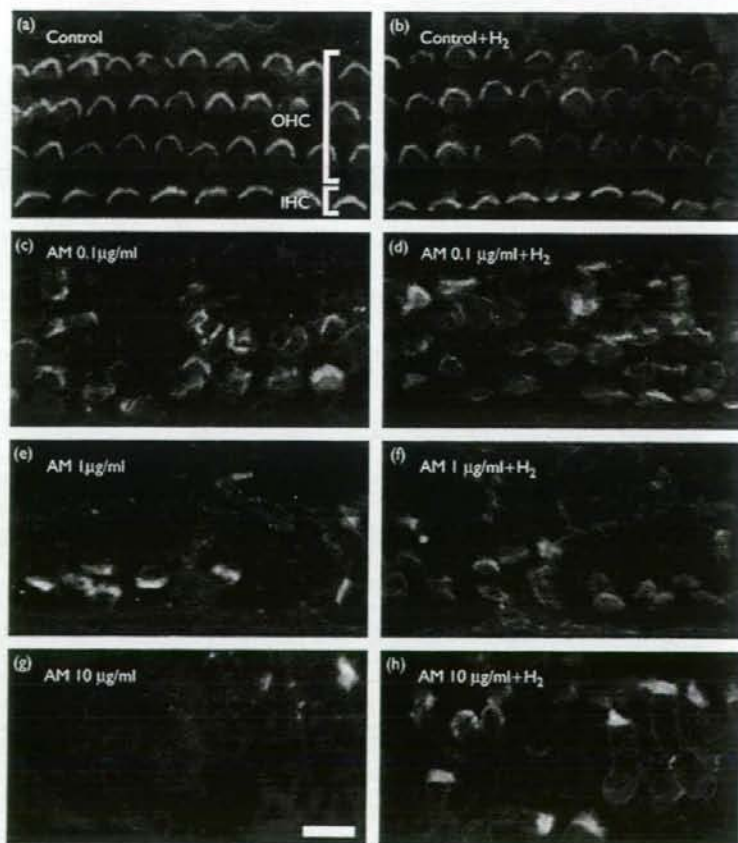
Effect of hydrogen on the survival of cochlear hair cells. (a–h) Photomicrographs of phalloidin (green) and myosin VIIa (red)-labeled cochlear cultures, treated with 0 (a and b), 0.1 (c and d), 1 (e and f), and 10 μg/ml (g and h) antimycin A (AM), with (b, d, f and h) or without (a, c, e and g) hydrogen gas (H₂). Bar, 5 μm. IHCs, inner hair cells; OHCs, outer hair cells.

showed that the loss of OHCs was significantly lower ($P < 0.01$) in the groups treated with 0.1 µg/ml antimycin A and hydrogen than in the groups treated with antimycin A alone (Fig. 3). These data showed that hydrogen protected hair cells against antimycin A-induced toxicity in this model of cochlear damage.

Reactive oxygen species reduction by molecular hydrogen
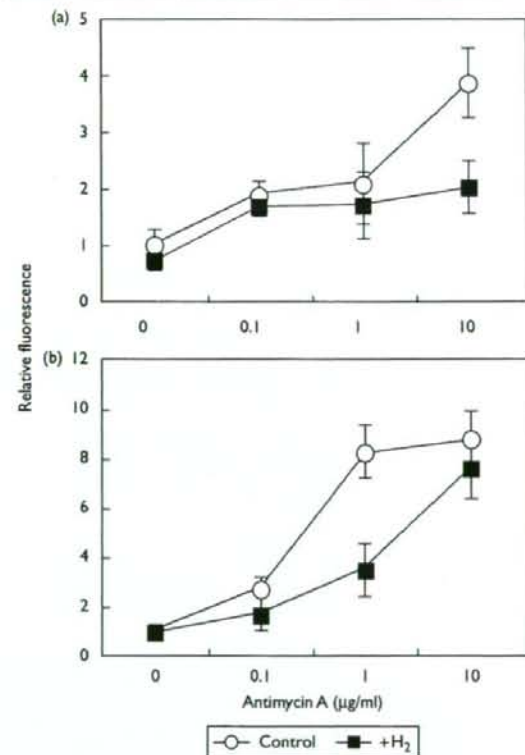To investigate the mechanism by which hydrogen alleviated hair-cell damage, we measured the ROS production in the cochlear cultures (Fig. 3). HPF is a reagent that was developed to detect certain highly ROS directly [16]. In cochlear cultures treated with 0–10 µg/ml antimycin A for 45 min, in the absence of hydrogen gas, the HPF signals increased (Fig. 4a), indicating that antimycin A induced the production of hydroxyl radicals. The intensity of the HPF fluorescence after the treatment with 10 µg/ml antimycin A was 3.61 times greater than that in the absence of antimycin A (Fig. 4a). By contrast, adding hydrogen gas to the cultures resulted in a reduction of the HPF signal intensity. In the

Fig. 3

Hair-cell counts in molecular hydrogen-treated cultures. After 24-h culture with antimycin A, inner hair cells (IHCs) (a) and outer hair cells (OHCs) (b) were counted. White box symbols represent the counts from control cultures without molecular hydrogen, and black symbols represent those from cultures with molecular hydrogen. Molecular hydrogen significantly attenuated the loss of IHCs ($P=0.0031$) and OHCs ($P=0.0016$) in antimycin A-damaged cochleae according to a two-way analysis of variance. Post hoc analyses with Tukey–Kramer tests for multiple paired comparisons showed that the OHC loss was significantly lower in cultures treated with antimycin A plus hydrogen gas than in those treated with 0.1 µg/ml antimycin A alone (*$P<0.01$). Bars represent standard errors.

Fig. 4

Molecular hydrogen reduced reactive oxygen species (ROS) production and lipid oxygenation. White circle symbols represent the counts from control cultures without molecular hydrogen, and black box symbols represent those from cultures with molecular hydrogen. (a) ROS production was measured in cultures treated with antimycin A with or without hydrogen gas for 40 min, according to the intensity of chemifluorescence of 2-[6-(4'-hydroxy)phenoxy-3H-xanthen-3-on-9-yl] benzoate (HPF). The relative HPF fluorescence intensity in the organ of Corti increased dose dependently in the presence of antimycin A, but was significantly reduced by the addition of hydrogen gas ($P=0.0439$). (b) Lipid oxygenation was measured in cultures treated with antimycin A with or without hydrogen gas for 24 h, according to the intensity of immunohistochemical labeling for 4-hydroxynonenal (HNE). The relative HNE-staining intensity in the organ of Corti increased dose dependently in the presence of antimycin A, but was significantly reduced by the addition of hydrogen gas ($P=0.0447$). Bars represent standard errors.

presence of hydrogen gas, the intensity of the HPF fluorescence after the treatment with 10 µg/ml antimycin A was 2.34 times greater than that in the absence of antimycin A (i.e. 52.1% of that without molecular hydrogen). Two-way ANOVA showed that hydrogen had a significant effect on the production of hydroxyl radicals ($P = 0.0439$). No significant differences were identified in multiple paired comparisons with Tukey–Kramer tests.

We also investigated the expression of HNE, which is a lipid-peroxidation marker, in the explant cultures. HNE production increased dose dependently in the presence of antimycin A. The intensity of the HNE fluorescence after the treatment with 10 µg/ml antimycin was 8.68 times greater than that in the absence of antimycin A (Fig. 4b). Adding molecular hydrogen to the cultures resulted in a significant reduction of HNE expression. Two-way ANOVA showed that hydrogen had a significant effect on the production of HNE ($P = 0.0446$), but, no significant differences were identified in multiple paired comparisons with Tukey–Kramer tests. Molecular hydrogen had its greatest effect at an antimycin concentration of 1 µg/ml, when the HNE production was attenuated to 42.4% of the level seen in the absence of molecular hydrogen.

Discussion

To our knowledge, this study was the first to evaluate the therapeutic potential of molecular hydrogen for the auditory system. A quantitative assessment of the hair-cell loss caused by antimycin A showed a dose-dependent effect, indicating that the toxic effects in this explant culture system represented a good model for the cochlea *in vivo*. Treating the cultures with hydrogen gas significantly influenced the dose response for hair-cell loss because of antimycin A, indicating that hydrogen gas has a protective effect on hair cells against ROS toxicity.

We also investigated the mechanisms by which hydrogen gas protected hair cells from damage in the cochlea. Our results showed that the hydrogen gas in fact reduced the production of cellular ROS and subsequent lipid oxygenation. Our antimycin A cochlea culture system, along with chemiluminescence detection, was shown to be useful in screening for antioxidant drugs, because antimycin A directly produces ROS in the cochlea and the direct measurement of ROS was possible when HPF was used.

Hydrogen is one of the most abundant and well-known molecules. Inhalation of hydrogen gas has been used in the prevention of decompression sickness in divers and has shown a good safety profile [8]. Hydrogen has been approved by the US Food and Drug Administration for the treatment of several different diseases. Ohsawa *et al.* [8] demonstrated that hydrogen gas is a potent anti-oxidant with certain unique properties. First, hydrogen gas is permeable to cell membranes and can target

organelles, including mitochondria and nuclei. Second, hydrogen gas specifically quenches detrimental ROS, such as the hydroxyl radical and peroxynitrite, while maintaining the metabolic oxidation–reduction reaction and other less-potent ROS, such as hydrogen peroxide and nitric oxide. The first feature is especially favorable in inner-ear medicine, because many therapeutic compounds are blocked by the blood–cochlear barrier and cannot reach cochlear hair cells [17,18]. Therefore, hydrogen therapy could be widely used in medical applications as a safe and effective antioxidant with minimal side effects.

Conclusion

In conclusion, this study showed that hydrogen gas markedly decreased oxidative stress by scavenging ROS, and protected cochlear cells and tissues against oxidative stress. These results have prompted us to perform in-vivo studies to determine whether treatment with hydrogen gas might exert a beneficial effect on damaged cochleae and promote hearing recovery.

References
1 Jiang H, Talaska AE, Schacht J, Sha SH. Oxidative imbalance in the aging inner ear. *Neurobiol Aging* 2007; **28**:1605–1612.
2 Yamane H, Nakai Y, Takayama M, Iguchi H, Nakagawa T, Kojima A. Appearance of free radicals in the guinea pig inner ear after noise-induced acoustic trauma. *Eur Arch Otorhinolaryngol* 1995; **252**:504–508.
3 Yamashita D, Jiang HY, Schacht J, Miller JM. Delayed production of free radicals following noise exposure. *Brain Res* 2004; **1019**:201–209.
4 Lee JE, Nakagawa T, Kim TS, Endo T, Shiga A, Iguchi F, *et al.* Role of reactive radicals in degeneration of the auditory system of mice following cisplatin treatment. *Acta Otolaryngol* 2004; **124**:1131–1135.
5 Clerici WJ, Hensley K, DiMartino DL, Butterfield DA. Direct detection of ototoxicant-induced reactive oxygen species generation in cochlear explants. *Hear Res* 1996; **98**:116–124.
6 Linseman DA. Targeting oxidative stress for neuroprotection. *Antioxid Redox Signal* 2008; ■:■–■. Aug 20. [Epub ahead of print]
7 Klein M, Koedel U, Pfister HW. Oxidative stress in pneumococcal meningitis: a future target for adjunctive therapy? *Prog Neurobiol* 2006; **80**:269–280.
8 Ohsawa I, Ishikawa M, Takahashi K, *et al.* Hydrogen acts as a therapeutic antioxidant by selectively reducing cytotoxic oxygen radicals. *Nat Med* 2007; **13**:688–694.
9 Fukuda K, Asoh S, Ishikawa M, Yamamoto Y, Ohsawa I, Ohta S. Inhalation of hydrogen gas suppresses hepatic injury caused by ischemia/reperfusion through reducing oxidative stress. *Biochem Biophys Res Commun* 2007; **361**:670–674.

10 Hayashida K, Sano M, Ohsawa I, Shinmura K, Tamaki K, Kimura K, et al. Inhalation of hydrogen gas reduces infarct size in the rat model of myocardial ischemia-reperfusion injury. *Biochem Biophys Res Commun* 2008; **373**:30–35.

11 Sato Y, Kajiyama S, Amano A, Kondo Y, Sasaki T, Handa S, et al. Hydrogen-rich pure water prevents superoxide formation in brain slices of vitamin C-depleted SMP30/GNL knockout mice. *Biochem Biophys Res Commun* 2008; **375**:346–350.

12 Nagata K, Nakashima-Kamimura N, Mikami T, Ohsawa I, Ohta S. Consumption of molecular hydrogen prevents the stress-induced impairments in hippocampus-dependent learning tasks during chronic physical restraint in mice. *Neuropsychopharmacology* 2008; **34**:501–508.

13 Kajiyama S, Hasegawa G, Asano M, Hosoda H, Fukui M, Nakamura N, et al. Supplementation of hydrogen-rich water improves lipid and glucose metabolism in patients with type 2 diabetes or impaired glucose tolerance. *Nutr Res* 2008; **28**:137–143.

14 Sha SH, Taylor R, Forge A, Schacht J. Differential vulnerability of basal and apical hair cells is based on intrinsic susceptibility to free radicals. *Hear Res* 2001; **155**:1–8.

15 Futai N, Gu W, Song JW, Takayama S. Handheld recirculation system and customized media for microfluidic cell culture. *Lab Chip* 2006; **6**:149–154.

16 Setsukinai K, Urano Y, Kakinuma K, Majima HJ, Nagano T. Development of novel fluorescence probes that can reliably detect reactive oxygen species and distinguish specific species. *J Biol Chem* 2003; **278**:3170–3175.

17 Coimbra RS, Loquet G, Leib SL. Limited efficacy of adjuvant therapy with dexamethasone in preventing hearing loss due to experimental pneumococcal meningitis in the infant rat. *Pediatr Res* 2007; **62**:291–294.

18 Laurell GF, Teixeira M, Duan M, Sterkers O, Ferrary E. Intact blood-perilymph barrier in the rat after impulse noise trauma. *Acta Otolaryngol* 2008; **128**:608–612.